

Cite this: *Dalton Trans.*, 2019, **48**, 9127Received 15th February 2019,
Accepted 23rd May 2019

DOI: 10.1039/c9dt00702d

rsc.li/dalton

Reactivity of a gold(i)/platinum(0) frustrated Lewis pair with germanium and tin dihalides†

Nereida Hidalgo,^a Sonia Bajo,^a Juan José Moreno,^a Carlos Navarro-Gilabert,^a Brandon Q. Mercado^b and Jesús Campos^a

The reactivity of germanium and tin dichlorides with a transition metal-only frustrated Lewis pair based on Au(I) and Pt(0) compounds bearing bulky phosphine ligands is described in this work. We have examined both the reactivity of tetrylene dihalides towards the individual components of the metallic pair, as well as under metal/metal cooperative conditions. These studies allowed us to isolate several uncommon homo- and heterometallic structures. Computational methods have been employed to investigate the bonding scheme of one of these highly-reduced metallic aggregates. In addition, we have developed a tin-promoted strategy to access heteroleptic diphosphine platinum(0) compounds.

Introduction

The use of molecular donor-acceptor pairs has served as a fruitful tool to stabilize or intercept reactive inorganic species with ambiphilic character.¹ The strategy has been particularly successful in the study of heavier tetrylenes, :EX₂ (E = Si, Ge, Sn, Pb), compounds based on a divalent heavier group 14 element, which possess relatively reduced HOMO-LUMO gaps and dual nucleophilic (lone electron pair) and electrophilic (empty p orbital) nature. The cooperative stabilization conferred by a donor and an acceptor that mutually bind an ambiphilic molecule is understood in terms of the electronic push-pull bonding scheme that emerges. Representative examples of otherwise highly unstable tetrylene fragments include E(CH₃)₂,² EH₂,³ or SiCl₂,⁴ which have been characterized by this approach, providing fundamental understanding of their bonding and reactivity. Stabilizing heavier tetrylenes by intra- or intermolecular donors has also been exploited in their use as more robust ligands in coordination chemistry.⁵

From a related perspective, this electronic push-pull stabilization highly resembles the chemistry of frustrated Lewis pairs (FLPs). These systems have been widely employed to capture an ample range of small molecules by the synergistic

combination of an acid and a base for which adduct formation has been quenched.⁶ However, the presence of heavier group 14 elements within the field of FLPs mostly focuses on their use as acidic partners,⁷ while reactivity studies of traditional FLP systems towards the tetrel series finds little precedent.⁸ We recently entered the FLP arena by describing the first transition metal-only FLP (TMOFLP) in which the two constituents were based on transition metals, more precisely Au(I) and Pt(0) as the acidic and basic counterparts respectively (Fig. 1).⁹ Somehow related metal-only donor-acceptor pairs (Rh/W and Pt/W) have been recently employed by Rivard to stabilize low-valent group 14 species.¹⁰ Encouraged by these results we decided to explore the reactivity of our Au(I)/Pt(0) FLP towards simple forms of low-valent group 14 compounds, particularly GeCl₂ and SnCl₂. It is pertinent to note that after push-pull stabilization, germanium and tin dihalides could serve as suitable precursors towards their corresponding dialkyl² or dihydride³ derivatives, which in turn can be the source of functional nanomaterials.¹¹ We will firstly present the reactivity of

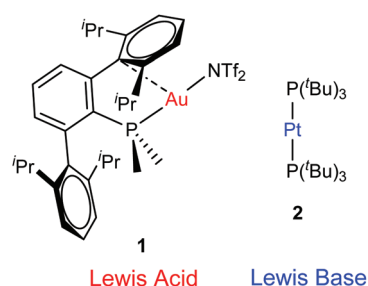


Fig. 1 Transition metal-only frustrated Lewis pair (TMOFLP) studied in this work, where the weakly coordinating triflimide anion ($[\text{N}(\text{SO}_2\text{CF}_3)_2]^-$) is represented by NTf_2^- .

^aInstituto de Investigaciones Químicas (IIQ), Departamento de Química Inorgánica and Centro de Innovación en Química Avanzada (ORFEO-CINQA), Universidad de Sevilla and Consejo Superior de Investigaciones Científicas (CSIC), Avenida América Vespucio 49, 41092 Sevilla, Spain. E-mail: jesus.campos@iiq.csic.es

^bDepartment of Chemistry, Yale University, 225 Prospect St, New Haven, CT 06511, USA

† Electronic supplementary information (ESI) available: Synthetic procedures and characterization of new compounds, crystallographic and computational details and NMR and HRMS spectra. CCDC 1897306–1897311. For ESI and crystallographic data in CIF or other electronic format see DOI: 10.1039/c9dt00702d

germanium and tin dihalides with the gold and platinum single components of the FLP. The discussion will then be continued by describing their combined reactivity. In addition, the present studies reveal the key role of tin dichloride in promoting phosphine exchange reactions for the platinum component of the metallic FLP.

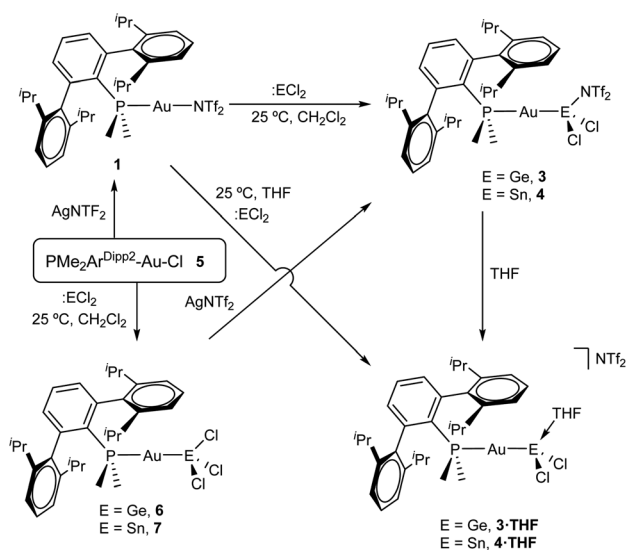
Results and discussion

Reactivity of GeCl_2 and SnCl_2 towards gold compound **1**

We began our studies by exploring the reactivity of germanium and tin dihalides towards gold compound $(\text{PMe}_2\text{Ar}^{\text{Dipp}_2})\text{Au}(\text{NTf}_2)$, **1**. In both cases reactions proceed readily to yield compounds **3** and **4** after the respective insertion of GeCl_2 or SnCl_2 into the $\text{Au}-\text{N}(\text{SO}_2\text{CF}_3)_2$ bond of **1** (Scheme 1) in quantitative spectroscopic yield. These species were isolated as white powders and their purity confirmed by microanalysis. While **3** features a broad $^{31}\text{P}\{^1\text{H}\}$ NMR resonance in CD_2Cl_2 at 4.8 ppm, shifted to higher frequency by about 16 ppm relative to **1** ($\delta = -11.5$ ppm), the analogous broad signal due to **4** appears at -9.3 ppm. These resonances become sharp upon cooling the NMR probe to -40 °C suggesting fluxional behaviour for both compounds likely due to the lability of the triflimide anion. Similarly, all the resonances observed in their ^1H NMR spectra become sharper when recorded at low temperatures and do not exhibit any relevant features that differ from those of precursor **1**. Fluxional behaviour seems to be hampered in THF- d_8 solution, where the $^{31}\text{P}\{^1\text{H}\}$ NMR resonances of the gold germyl and stannyl compounds shift to higher frequencies (**3**·THF, 6.7 ppm; **4**·THF, -3.1 ppm) likely due to the displacement of the weakly coordinating triflimide anion by a solvent molecule (Scheme 1). As introduced above, the bonding scheme in these cationic complexes may be understood in terms of the push-pull interactions provided by the Au/THF

pair to the $:\text{ECl}_2$ moiety. However, while **4**·THF remains stable in solution for at least one day, its germanium analogue is acidic enough to readily promote the electrophilic ring-opening polymerization of THF.¹²

Despite our efforts, we were unable to grow single crystals of enough quality to authenticate the proposed formulation for compounds **3** and **4**. Nevertheless, the insertion of germynes and stannylenes into gold-halide and other related bonds is well-documented. In fact, the same reactivity is observed when GeCl_2 -dioxane or SnCl_2 are added to dichloromethane solutions of the gold chloride compound $(\text{PMe}_2\text{Ar}^{\text{Dipp}_2})\text{AuCl}$ (**5**),¹³ precursor of **1** via salt metathesis with AgNTf_2 (Scheme 1). The resulting gold-tetryl species are characterized by $^{31}\text{P}\{^1\text{H}\}$ NMR resonances at 5.0 and -2.2 ppm due to the germyl (**6**) and stannyl (**7**) insertion products respectively, while their ^1H NMR spectra match with those of their precursor **5**, as well as with other gold derivatives previously described by some of us.¹³ Subsequent chloride abstraction by silver triflimide results in quantitative formation of compounds **3** and **4**, respectively, as expected for the proposed molecular formulations collected in Scheme 1. The insertion of tetrylenes into gold-halide bonds has provided complexes with Au-E (E = Ge, Sn) bonds with a variety of geometries and coordination environments,¹⁴ as well as interesting photophysical properties.¹⁵ Most examples rely on the use of sterically unhindered phosphines that permit the formation of supramolecular aggregates by aurophilic and other non-covalent interactions. The former interactions have indeed been suggested as key for the reported photoluminescent properties of these species. The solid-state structure of complex **6** is depicted in Fig. 2, revealing that no gold aggregates are formed. At variance with prior examples, gold-gold and gold-chloride contacts are replaced by a weak $\text{Au}\cdots\text{C}_{\text{arene}}$ interaction with the *ipso* carbon of a lateral terphenyl ring ($d_{\text{Au}\cdots\text{C}_{\text{ipso}}} = 2.95(4)$ Å), a common feature for gold complexes of biaryl phosphines.^{13,16} This forces the coordination geometry around gold to bend from linearity ($\text{P}-\text{Au}-\text{Ge}$ 171.30(4)°), while other



Scheme 1 Reactivity of tetrylene dihalides with gold compounds bearing a terphenyl phosphine.



Fig. 2 ORTEP diagram of compound **6**; for the sake of clarity hydrogen atoms are excluded and some substituents have been represented in wireframe format, while thermal ellipsoids are set at 50% probability.



distances and angles lie within normal values. The two flanking aryl rings of the terphenyl fragment are equivalent by NMR, while the $^{13}\text{C}\{^1\text{H}\}$ NMR resonance of the interacting *ipso*-carbon (138.1 ppm, $^3J_{\text{CP}} = 6$ Hz) lies close to the analogous one in the free phosphine (142.5 ppm, $^3J_{\text{CP}} = 5$ Hz). This data, along with the long $\text{Au}\cdots\text{C}_{\text{Arene}}$ distance, suggests that the secondary interaction is weak. For the sake of comparison, we aimed to examine the supramolecular structure of a compound analogous to **6** but constructed around the less hindered terphenyl phosphine $\text{PMe}_2\text{Ar}^{\text{Xyl}}_2$ (where $\text{Ar}^{\text{Xyl}}_2 = \text{C}_6\text{H}_3-2,6-(\text{C}_6\text{H}_3-2,6-\text{Me}_2)_2$), in which the isopropyl groups of the lateral aryl rings were replaced by methyl groups. The related gold germyl compound was prepared in good yields (*ca.* 90%) by the same strategy followed to access its bulkier counterpart (see ESI† for details). Its solid-state structure was almost identical to **6** and exhibits a similar secondary Au–arene interaction characterized by a $d_{\text{Au}-\text{C}_{\text{ipso}}}$ of 3.05(4) Å and a reduced P–Au–Ge angle of 165.77(2)° (Fig. S1†).

Drawing on the same theme, we wondered if the steric properties of terphenyl phosphines would still permit the insertion of bulkier tetraalkyls across the gold-chloride/triflimide bond.¹⁷ We chose stannylene $\text{Sn}[\text{N}(\text{SiMe}_3)_2]$ to carry out these experiments since its insertion into Au–Cl bonds was recently documented.^{17b} Its addition to benzene solutions of **1** and **5** indeed resulted in almost quantitative formation of compounds **9** and **8**, respectively (Scheme 2). Trace amounts of another gold complex were detected, as discussed below. The new Au–Sn heterobimetallic compounds are characterized by a higher-frequency shift of their $^{31}\text{P}\{^1\text{H}\}$ NMR resonances (**8**, 15.4 ppm; **9**, 13.8 ppm) of around 23 ppm with respect to their precursors. The $^{31}\text{P}\{^1\text{H}\}$ NMR signal of compound **8** exhibits a strong two-bond coupling due to the *trans* tin centre ($^2J_{\text{Psn}} = 3201$ Hz). A new intense signal in the ^1H NMR spectrum is collected at around 0.47 ppm due to the trimethylsilyl groups for both **8** and **9**, while the rest of their ^1H NMR spectra is comparable to other related samples described herein. Authenticating the proposed molecular structures proved challenging due to the poor quality of the crystals grown with the selected phosphine system. However, we succeeded in growing crystals with a related bulkier phosphine, namely $\text{PCyp}_2\text{Ar}^{\text{Xyl}}_2$ (Cyp = C_5H_9). Thus, compound **8**^{Cyp} was isolated in moderate yield as a white crystalline material following the same synthetic procedure described to access **8** (see Experimental section). Its $^{31}\text{P}\{^1\text{H}\}$ NMR resonance displays a $^2J_{\text{Psn}}$ coupling constant of 2846 Hz, somewhat smaller relative to compound

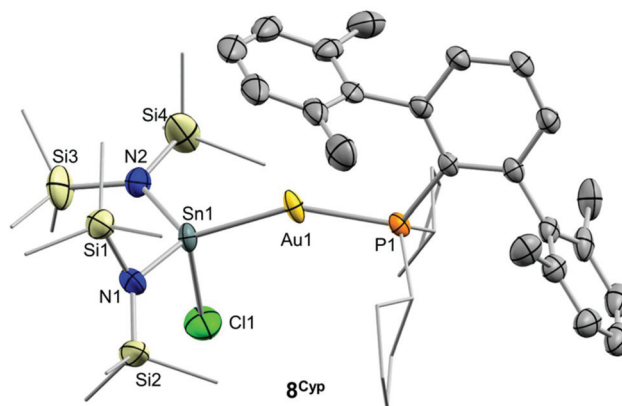


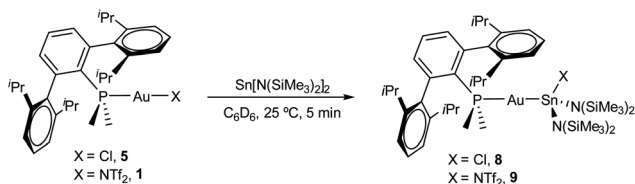
Fig. 3 ORTEP diagram of compound **8**^{Cyp}; for the sake of clarity hydrogen atoms are excluded and some substituents have been represented in wireframe format, while thermal ellipsoids are set at 50% probability.

8. This may result from the steric pressure exerted by the cyclopentyl substituents of the phosphorus centre onto the bulky bis(trimethylsilyl)amido fragments, which could weaken the metal–metal bond. In fact, its X-ray diffraction structure (Fig. 3) reveals a Au–Sn bond distance that accounts for 2.65(1) Å, relatively elongated compared to previous linear gold–tin complexes (*ca.* 2.57 Å).¹⁸

In addition, we could isolate the main side product resulting from the reactions represented in Scheme 2 (<5% by $^{31}\text{P}\{^1\text{H}\}$ NMR spectroscopy), which consists of an amido-bridged cationic digold complex of formula $[\text{Au}_2(\mu\text{-N}(\text{SiMe}_3)_2)(\text{PMe}_2\text{Ar}^{\text{Dipp}^2})_2]$ (see ESI† for details) due to the transfer of a trimethylsilylamido substituent from stannylene to a gold centre. This compound could be independently synthesized by mixing equimolar amounts of gold-triflimide **1** and $[\text{PMe}_2\text{Ar}^{\text{Dipp}^2}]_2\text{Au}[\text{N}(\text{SiMe}_3)_2]$, prepared by reaction of gold-chloride **5** and $\text{Li}[\text{N}(\text{SiMe}_3)_2]$. The molecular formulation of the amido-bridged digold compound based on $\text{PMe}_2\text{Ar}^{\text{Xyl}}_2$ phosphine was further confirmed by single-crystal X-ray diffraction studies (Fig. S2†) and represents an uncommon example of this motif in the context of gold chemistry.¹⁹

Reactivity of GeCl_2 and SnCl_2 towards platinum compound **2**

The reaction of tetrel dihalides,²⁰ as well as aluminum trichloride,²¹ with linear platinum(0) compounds has been investigated by Braunschweig and co-workers. In those studies the reactions of $:\text{GeCl}_2$ and $:\text{SnCl}_2$ with $[\text{Pt}(\text{PCy}_3)_2]$ (Cy = cyclohexyl) yielded the corresponding mononuclear dihalogermylene and -stannylene compounds $(\text{PCy}_3)_2\text{Pt}=\text{ECl}_2$ (E = Ge, Sn). In stark contrast, reactions of equimolar amounts of $:\text{ECl}_2$ and $[\text{Pt}(\text{P}^t\text{Bu}_3)_2]$ (**2**) did not result in major alterations of the resonances recorded by ^1H and $^{31}\text{P}\{^1\text{H}\}$ NMR spectroscopy relative to reactant **2**, although a rapid colour change from colourless to dark red was noticeable in both cases. The dissimilar reactivity of compound **2** and its PCy_3 analogue towards $:\text{ECl}_2$ is reminiscent to their reaction with H_2 , which is rapid for $[\text{Pt}(\text{PCy}_3)_2]$ ²² but impracticable for **2** unless gold complex **1** is present, in which case an FLP-like H_2 splitting takes place.⁹



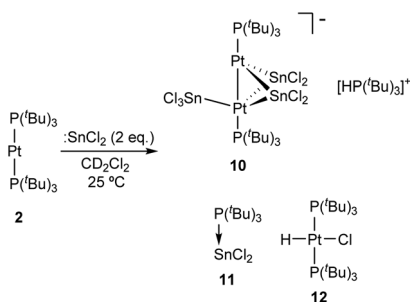
Scheme 2 Reaction of stannylene $\text{Sn}[\text{N}(\text{SiMe}_3)_2]$ with gold precursors **1** and **5**.



We ascribe the lack of reactivity of **2** to the high steric shielding provided by the *tert*-butyl phosphines.

Although the Pt(0) compound **2** remained practically unchanged, we observed a new $^{31}\text{P}\{^1\text{H}\}$ NMR signal at 94.5 ppm after the addition of one equivalent of $:\text{GeCl}_2$ -dioxane to its CD_2Cl_2 solution, but it accounted for only around 5% of the overall phosphorus content, preventing the observation of a ^{195}Pt - ^{31}P coupling constant. Based on its chemical shift and in comparison with prior studies by Braunschweig this signal could be tentatively assigned to a Pt germylene compound analogous to $(\text{PCy}_3)_2\text{Pt}=\text{GeCl}_2$.^{20b} However, addition of excess $:\text{GeCl}_2$ did not lead to a major increase in the proportion of this species, which remained as the minor product (<10%) under all attempted conditions. We decided to examine whether an equilibrium towards the formation of a Pt germylene could be observed at variable temperature. Low-temperature multinuclear NMR spectroscopic studies revealed dynamic behaviour in solution, although the proportion of the suggested Pt germylene remained practically unaltered. However, an additional broad $^{31}\text{P}\{^1\text{H}\}$ NMR resonance at 119.4 ppm exhibiting a large $^1J_{\text{PPT}}$ coupling constant of 4670 Hz became discernible below -20°C and reached a proportion of around 20% at -60°C . Although we are unsure of the nature of this new species, it seems to result from the dissociation of a phosphine ligand, as evinced by a $^{31}\text{P}\{^1\text{H}\}$ NMR signal at 59.9 ppm of intensity equal to the newly formed compound and corresponding to P^tBu_3 . Based on the analogous reactivity with $:\text{SnCl}_2$ (*vide infra*) we tentatively suggest the formation of a dinuclear platinum compound stabilized by bridging germanium halides.

Although treatment of CD_2Cl_2 solutions of **2** with equimolar amounts of $:\text{SnCl}_2$ led to an immediate colour change to dark red, we could not observe the formation of Pt stannylene or the existence of an equilibrium with such a species by low-temperature ^1H and $^{31}\text{P}\{^1\text{H}\}$ NMR monitoring. Identical results were derived from reactions in tetrahydrofuran where tin dichloride exhibits better solubility. In contrast, the addition of a second equivalent of $:\text{SnCl}_2$ in chlorinated solutions drastically changed the reaction outcome. Complete disappearance of Pt(0) compound **2** is immediately recorded upon addition of the second equivalent of tin dichloride at room temperature to yield a complex mixture of species, in which we could unambiguously identify several platinum compounds (Scheme 3). A



Scheme 3 Reactivity of Pt(0) compound **2** with 2 equivalents of $:\text{SnCl}_2$.

$^{31}\text{P}\{^1\text{H}\}$ NMR resonance recorded at 52.8 ppm and exhibiting a $^1J_{\text{PSn}}$ coupling-constant of 1855 Hz accounts for the formation of the tin-phosphine adduct **11**, confirmed by the independent reaction between $:\text{SnCl}_2$ and P^tBu_3 . It is worth mentioning that in all experiments described herein variable amounts of $[\text{PtClH}(\text{P}^t\text{Bu}_3)_2]$ (**12**) were formed, likely due to reaction of **2** with hydrochloric acid produced by adventitious traces of water in the presence of $:\text{SnCl}_2$. Phosphonium cation $[\text{H}(\text{P}^t\text{Bu}_3)]^+$ was produced by the same reason and displays a distinctive ^1H NMR doublet at 6.02 ppm ($^1J_{\text{HP}} = 408$ Hz). More interestingly, the higher-frequency region of the $^{31}\text{P}\{^1\text{H}\}$ NMR spectra reveals the formation of a major compound (**10**) that resonates at 128.3 ppm and is accompanied by both ^{119}Sn ($^2J_{\text{PSn}} = 110$ Hz) and ^{195}Pt ($^1J_{\text{PPT}} = 4874$ Hz) satellites. We managed to grow crystals from the crude dichloromethane reaction mixtures that exhibit an intense dark red colour by slow diffusion of pentane at -30°C . X-ray diffraction studies proved the formation of a dinuclear Pt(0) compound **10** in which each metal bears a single tri(*tert*-butyl)phosphine ligand. The capacity of tin chloride to promote phosphine dissociation has been examined in more detail and will be discussed later. The dinuclear platinum fragment in **10** is held together by three tin chloride units, one of which formally appears as an anionic bridging stannyl fragment. A phosphonium cation $[\text{H}(\text{P}^t\text{Bu}_3)]^+$ linked to the Pt-cluster by $\text{P}-\text{H}^+\cdots\text{Cl}$ interactions (average $d_{\text{H}-\text{Cl}}$ 3.0 Å) compensates the anionic character of the Pt_2Sn_3 cluster. The anionic part of the molecular structure depicted in Fig. 4 can be described as a distorted trigonal bipyramid with a missing Pt-Sn edge and characterized by a Pt-Pt distance of 2.706(1) Å. The average Pt-Sn bond distances accounts for 2.58 Å, except for the SnCl_3^- termini, for which one of the two Pt-Sn contacts is



Fig. 4 ORTEP diagram of compound **10**; for the sake of clarity most hydrogens have been omitted and *tert*-butyl substituents have been represented in wireframe format. Thermal ellipsoids are set at 50% probability.



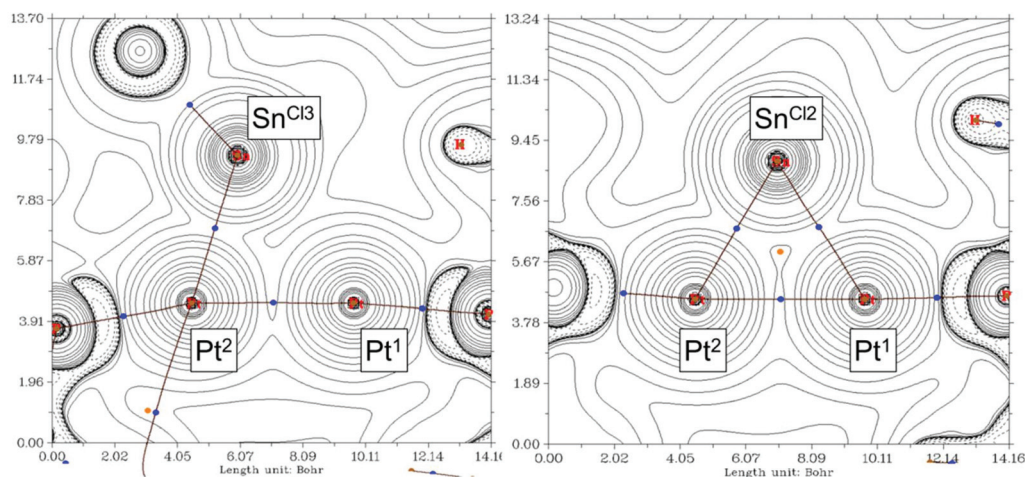


Fig. 5 Plot of the laplacian of the electron density, $\nabla^2\rho$, of complex **10** in the Pt(1)–Pt(2)–SnCl₃ (left) and the Pt(1)–Pt(2)–SnCl₂ (right) planes calculated with the ω B97X-D functional. The solid and dashed lines correspond to positive and negative values of $\nabla^2\rho$, respectively. In plane BCPs and BPs of the electron density are superimposed.

elongated to 2.998(2) Å. The P–Pt–Pt–P escapes from linearity due to the presence of the stannyl-bridged group, which distorts the ideal symmetry. Thus, one of the phosphine ligands tilts to accommodate the SnCl₃[−] group resulting in a Pt–Pt–P bond angle of 171.2 Å. A somehow related structure has been previously described in which the bridging divalent tin nuclei are stabilized by acetylacetonate ligands.²³ As in prior cases, the highly reduced character of the heteropolymetallic cluster is likely responsible for its high instability.²⁴

We found of interest to interrogate the bonding scheme in diplatinum **10** by computational methods. Optimization of its molecular geometry at the ω B97XD/6-31G(d,p) level of theory was in agreement with the solid state structure, with Pt–Pt and Pt–Sn bond distances of 2.77 and 2.63–2.69 Å, respectively, except for the SnCl₃[−] group, for which one of the two Pt–Sn contacts is elongated to 3.21 Å. Analysis of the computed electron density (QTAIM) performed at the same level of theory disclosed bond critical points (BCPs) and the corresponding bond paths (BPs) connecting each SnCl₂ fragment to both Pt atoms, while the SnCl₃[−] group binds to a single Pt centre (Pt(2)) (Fig. 5). Additionally, one BCP was located at the path between the Pt atoms, supporting the bonding interaction suggested by the short solid state Pt–Pt distance.

The analysis of the electron density was complemented with an analysis of localized molecular orbitals to rationalize the interactions between the [Pt(P^tBu₃)], SnCl₂ and SnCl₃[−] fragments, following the Pipek–Mezey²⁵ and NBO criteria. Both localization schemes provide similar information revealing that the three SnCl_n fragments donate electron density to one of the platinum atoms, Pt(2), whereas Pt(1) acts as a donor by delocalizing d-electron density onto empty p orbitals of the two SnCl₂ fragments (Fig. 6a). Besides, Pt(1) also behaves as an acceptor, since the Pt–Pt interaction arises from electron delocalization from one d orbital on Pt(2) onto Pt(1) as seen in Fig. 6b. Overall, the bonding in compound **10** could be ration-

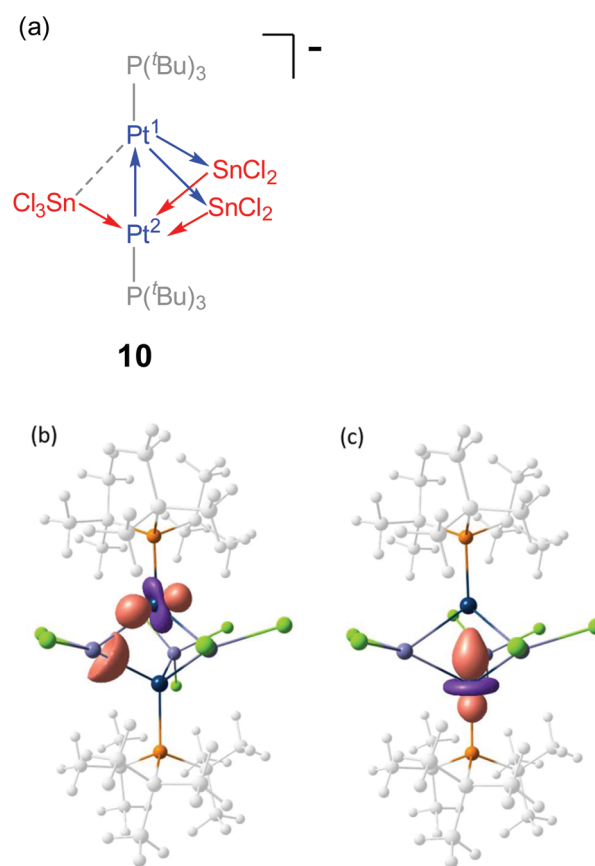


Fig. 6 (a) Simplified bonding scheme representation of compound **10**, where arrows describe electron donation between metal centres; (b, c) Representative localized molecular orbitals (Pipek–Mezey) involved in the Pt–Sn (b) and the Pt–Pt bonding (c).

alize by the schematic representation depicted in Fig. 6a, where each metal atom (except for SnCl₃[−]) exhibits ambiphilic donor–acceptor character.



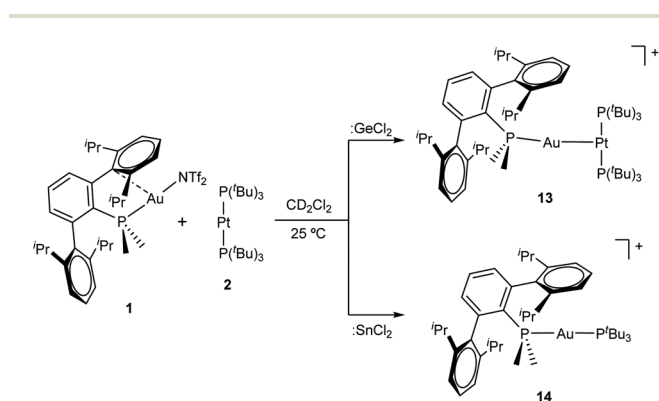
Reactivity of GeCl_2 and SnCl_2 towards a Au/Pt frustrated Lewis pair

After examining the reactivity of tetraylene dihalides with compounds **1** and **2** we moved to investigate their chemistry with the two metallic fragments in cooperation. Before describing the details of these experiments it must be noted that the reaction outcomes were independent of the order in which the three components were mixed together. In other words, the reaction of platinum compound **2** with pre-formed germyl or stannyl derivatives **3** and **4**, respectively, led to identical product distributions than those detected after the addition of gold compound **1** to dichloromethane solutions of **2** and the corresponding tetraylene. We previously showed that TMOFLP **1/2** exists in solution as an equilibrium between the independent metallic fragments and a metal-only Lewis pair (MOLP)²⁶ in which the electron-rich platinum forms a dative bond with the electrophilic gold nucleus. Although we could not detect the metallic Pt→Au adduct by spectroscopic methods, NMR line-broadening upon mixing **1** and **2** supported this assumption, with the prevalence of the individual components relative to the metallic adduct being ascribed to steric frustration.

To our surprise, treatment of dichloromethane solutions of the **1/2** pair with one equivalent of $:\text{GeCl}_2$ -dioxane cleanly generated the metallic adduct whose existence we had previously proposed⁹ (compound **13** in Scheme 4). The tetraylene seems to be key in withdrawing the triflimide anion from gold, likely by formation of $\text{NTf}_2 \rightarrow \text{GeCl}_2$. The formulation of the unsupported heterobimetallic compound **13** was ascertained by NMR spectroscopy and validated by microanalysis. In the $^{31}\text{P}\{^1\text{H}\}$ NMR spectrum a doublet at 94.5 ppm ($^1J_{\text{PPt}} = 3159$ Hz) with a small $^3J_{\text{PP}}$ coupling constant of 2 Hz was accompanied by a triplet at -34.2 ppm, highly shifted to lower frequencies with respect to gold compound **1** ($\delta = -11.5$ ppm) and also exhibiting an identical coupling constant of 2 Hz. Besides, the latter signal arises from the phosphine directly bound to the gold centre but features a relatively strong coupling to platinum ($^2J_{\text{PPt}} = 1984$ Hz). This $^{31}\text{P}\{^1\text{H}\}$ NMR pattern supports the fact that a new Pt→Au dative bond is present in compound **13**. The proposed molecular structure was also authenticated

by single-crystal X-ray diffraction studies. The triflimide salt of compound **13** co-crystallized with half a molecule of $[(\text{PMe}_2\text{Ar}^{\text{DippP}_2})_2\text{Au}]^+$ cation per asymmetric unit, as well as with another half a molecule of triflimide as counteranion. This is not surprising since cationic diphosphine gold species have been described as recurrent side-products in gold chemistry,²⁷ although its presence in solution was minimal (*ca.* 5%) as monitored by NMR spectroscopic techniques. The molecular structure of compound **13** is represented in Fig. 7. The platinum centre exhibits a slightly distorted T-shaped coordination environment, with a relatively reduced P–Pt–P bond of $167.59(5)^\circ$ likely due to the bulkiness of the $\text{Au}(\text{PMe}_2\text{Ar}^{\text{DippP}_2})$ unit bound to the Pt(0) centre. The Pt–Au distance amounts to $2.575(1)$ Å, significantly shortened when compared to its related heterobimetallic dihydride compound,⁹ but marginally longer than in compound $[(\text{PCy}_3)_2\text{Pt}] \rightarrow \text{Au}(\text{PCy}_3)$ ($d_{\text{Au–Pt}} = 2.54$ Å), the only other unsupported Pt(0)–Au(I) species structurally characterized to date.²⁸

As briefly noted earlier, compound **13** was alternatively synthesized by treatment of gold germyl **3** with $[\text{Pt}(\text{P}^t\text{Bu}_3)_2]$ **2**, which reflects the lability of the Au–Ge bond in these species. However, the reactivity of $:\text{SnCl}_2$ with Au/Pt **1/2** pair markedly differs and no metal-only Lewis adduct **13** was detected in any of our experiments. Instead, tin dichloride promoted an interesting phosphine exchange to yield the heteroleptic compound $[(\text{PMe}_2\text{Ar}^{\text{DippP}_2})\text{Au}(\text{P}^t\text{Bu}_3)]^+$ (**14**) as the only gold-containing species. $^{31}\text{P}\{^1\text{H}\}$ NMR spectroscopy revealed the immediate formation of compound **14** upon mixing the three reaction components, as evidenced by two set of doublets at 100.6 and 14.6 ppm, characterized by a two-bond coupling-constant of 312 Hz, analogous to other cationic and heteroleptic diphosphine gold derivatives.²⁹ We could not observe, however, any other signal by $^{31}\text{P}\{^1\text{H}\}$ NMR corresponding to the remaining Pt-bound tri-*tert*-butylphosphine.



Scheme 4 Combined reactivity of compounds **1** and **2** towards germanium and tin dihalides.

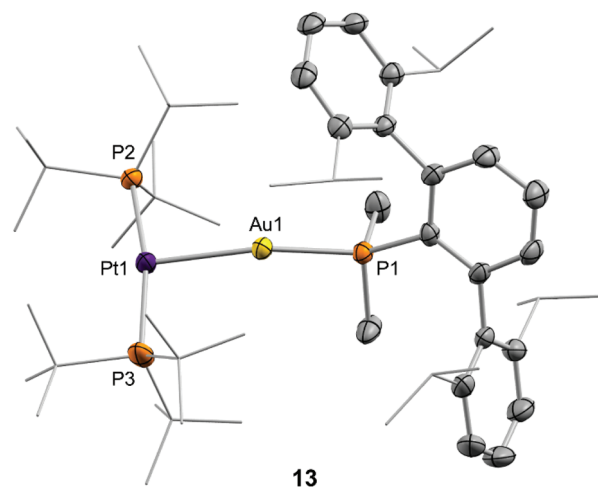


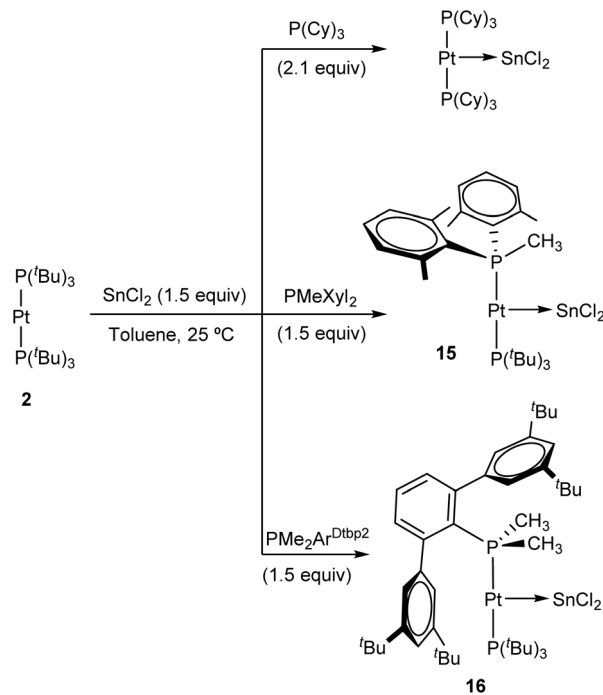
Fig. 7 ORTEP diagram of the cation of complex **13**; hydrogen atoms, half molecule of $[(\text{PMe}_2\text{Ar}^{\text{DippP}_2})_2\text{Au}]^+$ and triflimide anions are excluded for clarity and thermal ellipsoids are set at 50% probability. *tert*-Butyl and iso-propyl substituents have been drawn in wireframe format.



Tin-promoted phosphine exchange reactions

The ability of :SnCl_2 to mediate the transfer of a phosphine ligand from $\text{Pt}(0)$ to $\text{Au}(i)$ prompted us to investigate the possibility of accessing heteroleptic diphosphine $\text{Pt}(0)$ compounds, of which there are very few reported examples.³⁰ Prior studies have shown that ligand-exchange reactions between $[\text{Pt}(\text{PCy}_3)_2]$ and several *N*-heterocyclic carbenes (NHCs) provide access to heteroleptic NHC- Pt - PCy_3 derivatives,³¹ but the analogous substitution reaction to incorporate bulky phosphines into $\text{P}-\text{Pt}(0)-\text{P}'$ structures remains unknown. To carry out these studies we chose three bulky phosphines, more precisely PCy_3 , whose stannylene-platinum chemistry has already been outlined,³¹ as well as PMeXyl_2 ($\text{Xyl} = 2,6\text{-Me}_2\text{C}_6\text{H}_3$) and $\text{PMe}_2\text{Ar}^{\text{Dtbp}_2}$ ($\text{Ar}^{\text{Dtbp}_2} = \text{C}_6\text{H}_3\text{-}2,6\text{-(C}_6\text{H}_3\text{-}3,5\text{-(CMe}_3)_2$)), whose coordination chemistry and reactivity has been reported by our group.³² The progress of the exchange reactions can be easily monitored by $^{31}\text{P}\{^1\text{H}\}$ NMR spectroscopy. Heating equimolar solutions of $\text{Pt}(0)$ compound **2** and each of the three aforementioned phosphine ligands at 80°C for several days did not result in any apparent transformation in view of the resulting NMR spectra, except for PCy_3 , where minor amounts of unknown species were detected. Likewise, the inertness of **2** towards ligand substitution stands unaltered under excess of the free phosphine (up to 10 equivalents). In stark contrast, the addition of one equivalent of :SnCl_2 to the previous solutions led to rapid phosphine-exchange reactions that had in common the appearance of free P^tBu_3 as the main side-product. Best yields were obtained by the use of 1.5 equivalents of :SnCl_2 . In the case of PCy_3 , instead of the aimed heteroleptic $\text{Pt}(0)$ compound, immediate formation of $(\text{PCy}_3)_2\text{Pt}=\text{SnCl}_2$ at 25°C was evinced by $^{31}\text{P}\{^1\text{H}\}$ NMR spectroscopy (Scheme 5). A characteristic broad singlet at 51.4 ppm flanked by ^{195}Pt satellites ($^1J_{\text{Pt}} = 3525\text{ Hz}$), as previously described by Braunschweig,²⁰ demonstrated its formation, which became quantitative when performing the reaction with 2.1 equivalents of PCy_3 . The formation of unbound P^tBu_3 in a 1 : 2 ratio, with a $^{31}\text{P}\{^1\text{H}\}$ NMR signal at 59.9 ppm.

The reaction of PMeXyl_2 and $\text{Pt}(0)$ **2** in the presence of :SnCl_2 (1.5 equiv.) proceeds rapidly towards compound **15** in quantitative spectroscopic yield (Scheme 5). At variance with PCy_3 , the use of PMeXyl_2 permitted the formation of the desired heteroleptic $\text{Pt}(0)$ species in which only one of the two P^tBu_3 ligands was substituted by the incoming phosphine. In fact, using an excess of PMeXyl_2 did not lead to the homoleptic $\text{Pt}(0)$ compound analogous to $(\text{PCy}_3)_2\text{Pt}=\text{SnCl}_2$ even under moderate heating. The use of the bulkier phosphine $\text{PMe}_2\text{Ar}^{\text{Dtbp}_2}$ bearing a terphenyl group led to the formation of heteroleptic platinum stannylene **16** (Scheme 5), though it required longer reaction times. The high-resolution mass spectra of **15** and **16** fit exactly to their proposed formulation (see Experimental section and ESI[†]), albeit without the bound SnCl_2 fragment, not surprisingly given the lability of the $\text{Pt}\rightarrow\text{Sn}$ bond. Both compounds feature similar $^{31}\text{P}\{^1\text{H}\}$ NMR spectra characterized by two doublets exhibiting $^2J_{\text{PP}}$ of around 300 Hz, indicating the *trans* disposition of the two phosphines.



Scheme 5 Tin-mediated phosphine exchange reactions at $\text{Pt}(0)$ **2**.

Compound **15** leads to resonances at 94.6 and 6.3 ppm due to P^tBu_3 and PMeXyl_2 , respectively, while the analogous signals appear at 97.3 and 12.6 ppm due to P^tBu_3 and $\text{PMe}_2\text{Ar}^{\text{Dtbp}_2}$ in compound **16**. These resonances are flanked by ^{195}Pt satellites with strong coupling constants (**15**: $^1J_{\text{Pt}} = 3776$ and 3244 Hz ; **16**: $^1J_{\text{Pt}} = 3788$ and 3504 Hz). The presence of a tin centre bound to platinum was inferred in the two compounds from the satellites that escort the P^tBu_3 doublet ($^2J_{\text{PtSn}} \text{ ca. } 250\text{ Hz}$). In ^{195}Pt NMR spectra, their platinum centres resonate at about -5000 ppm as double doublets and, in the case of **15**, we could detect a large $^1J_{\text{PtSn}}$ coupling constant of 3210 that further corroborates the coordination of tin. Our attempts to record $^{119}\text{Sn}\{^1\text{H}\}$ NMR resonances were unsuccessful, though this is not unexpected due to the high asymmetry of the ^{119}Sn centres in these compounds, which results in an increased effect of chemical shift anisotropy in the relaxation of their NMR signals.³³ Coupling to the variety of neighbouring NMR-active nuclei adds to the difficulty of observing $^{119}\text{Sn}\{^1\text{H}\}$ NMR signals for **15** and **16**.

As a side note, we observed that the methyl group directly bound to the phosphorus centre in compound **15** resonates at 2.93 ppm (dd, $^3J_{\text{HPt}} = 50.7$, $^2J_{\text{HP}} = 9.0$, $^4J_{\text{HP}} = 2.5\text{ Hz}$) in the ^1H NMR spectrum, shifted to surprisingly higher frequency compared to free phosphine (1.63 ppm)³⁴ or to other $\text{Pt}-\text{PMeXyl}_2$ compounds previously reported by us (ca. 1.5–1.7 ppm).³³ However, its corresponding $^{13}\text{C}\{^1\text{H}\}$ resonance appears at 21.0 ppm ($^1J_{\text{CP}} = 37\text{ Hz}$), that is, within the expected range for a Ar_2PMe group. The unexpected ^1H NMR chemical shift served though to validate the proposed molecular structure of **15** by means of computational studies. A conformational analysis was calculated at the $\omega\text{B97XD}/6\text{-}31\text{G}(\text{d,p})$ level of theory



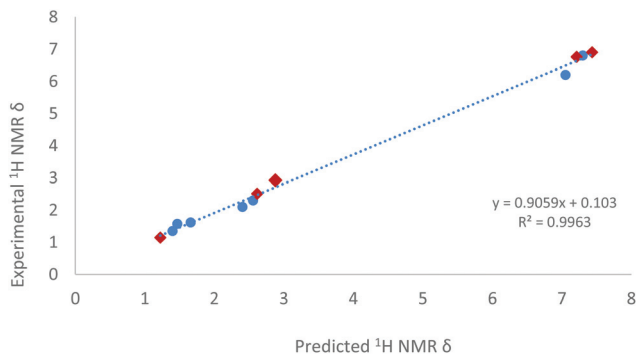


Fig. 8 Predicted and experimental ^1H NMR data relative to complexes **15** (red diamond), benchmarked against **2**, $[\text{Pt}(\text{PCy}_3)_2(\text{SnCl}_2)]^{20a}$ and $[\text{Pt}(\text{IMes})(\text{PCy}_3)(\text{SnCl}_2)]^{20a}$

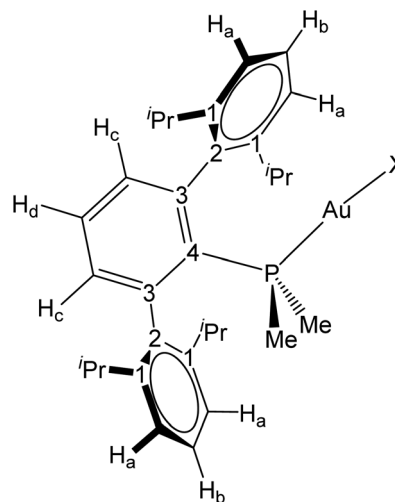


Fig. 9 Labeling scheme used for ^1H and $^{13}\text{C}\{^1\text{H}\}$ NMR assignments.

and disclosed no close contacts between the P-CH₃ moiety and the Sn or Pt centres. The geometric parameters of the minimum energy conformer of complex **15** (see Fig. S3†) are also comparable to previous platinum(0) diphosphine stannylene systems.²⁰ With this model in hand, we calculated the theoretical ^1H NMR chemical shifts of **15** by means of the GIAO method ($\omega\text{B97XD}/6\text{-311+G}(2\text{d,p})//\omega\text{B97XD}/6\text{-31G}(2\text{d,p})$).³⁵ To calibrate these results ^1H NMR data of compounds **2**, $[\text{Pt}(\text{PCy}_3)_2(\text{SnCl}_2)]^{20a}$ and $[\text{Pt}(\text{IMes})(\text{PCy}_3)(\text{SnCl}_2)]^{20a}$ (IMes = 1,3-dimesitylimidazol-2-ylidene) were also evaluated. The linear relationship found between calculated and experimental proton chemical shifts ($R^2 = 0.996$, Fig. 8) gives an expected δ of 2.71 ppm for the PMe moiety in complex **15**, in reasonable agreement with the experimental value (2.93 ppm).

Experimental section

General considerations

All preparations and manipulations were carried out using standard Schlenk and glove-box techniques, under an atmosphere of argon and of high purity nitrogen, respectively. All solvents were dried, stored over 4 Å molecular sieves, and degassed prior to use. Toluene (C₇H₈), *n*-pentane (C₅H₁₂) and *n*-hexane (C₆H₁₄) were distilled under nitrogen over sodium. Tetrahydrofuran (THF) and diethyl ether were distilled under nitrogen over sodium/benzophenone. [D₆]Benzene and [D₈]Toluene were distilled under argon over sodium/benzophenone, THF was dried over molecular sieves (4 Å) and CD₂Cl₂ over CaH₂ and distilled under argon. [AuCl(THT)] (THT = tetrahydrothiophene),³⁶ phosphine ligands $\text{PMe}_2\text{Ar}^{\text{Dipp}_2}$,¹³ $\text{PCyp}_2\text{Ar}^{\text{Xyl}_1}$,^{32c} $\text{PMe}_2\text{Ar}^{\text{Xyl}_2}$,^{33b} $\text{PMe}_2\text{Ar}^{\text{Dtbp}_2}$,^{32c} and compounds **1**,¹³ **2**,³⁷ and **5**¹³ were prepared as described previously. Other chemicals were commercially available and used as received. Solution NMR spectra were recorded on Bruker AMX-300, DRX-400 and DRX-500 spectrometers. Spectra were referenced to external SiMe₄ (δ : 0 ppm) using the residual proton solvent peaks as internal standards (^1H NMR experiments), or the characteristic resonances of the solvent nuclei (^{13}C NMR experiments), while ^{31}P and ^{195}Pt were referenced to H₃PO₄

and Na[PtCl₆], respectively. Spectral assignments were made by routine one- and two-dimensional NMR experiments where appropriate (Fig. 9). For elemental analyses a LECO TruSpec CHN elementary analyzer, was utilized. HRMS data were obtained on a JEOL JMS-SX 102A mass spectrometer by the Mass Spectrometry Services of the University of Seville (CITIUS).CCDC 1897306–1897311† (compounds **6**, **6**^{Xyl1}, **8**^{Cyp}, [Au₂(μ -N(SiMe₃)₂)(PMe₂Ar^{Xyl12})₂], **13**, **10**) contain the supplementary crystallographic data for this paper.

Compound 3

A solution of **1** (30 mg, 0.03 mmol) in CD₂Cl₂ (0.5 mL) was treated with :GeCl₂-dioxane (7.4 mg, 0.03 mmol) in a J. Young NMR tube. The tube was shaken resulting in the immediate formation of compound **3**, (15 mg, 46%). Anal. calcd for C₃₄H₄₃AuCl₂F₆GeNO₄PS₂: C, 37.8; H, 4.0; N, 1.3; S, 5.9. Found: C, 38.2; H, 4.2; N, 1.5; S, 5.5. ^1H NMR (400 MHz, CD₂Cl₂, 25 °C) δ : 7.60 (t, 1 H, $^3J_{\text{HH}} = 7.6$ Hz, H_d), 7.47 (t, 2 H, $^3J_{\text{HH}} = 7.6$ Hz, H_b), 7.4 (d, 4 H, $^3J_{\text{HH}} = 7.6$ Hz, H_a), 7.26 (dd, 2 H, $^3J_{\text{HH}} = 7.6$ Hz, $^4J_{\text{HP}} = 3.7$ Hz, H_c), 2.48 (sept, 4 H, $^3J_{\text{HH}} = 6.8$ Hz, $^1\text{Pr}(\text{CH})$), 1.37 (d, 6 H, $^2J_{\text{HP}} = 10$ Hz, PMe₂), 1.36 (d, 12 H, $^3J_{\text{HH}} = 6.8$ Hz, $^1\text{Pr}(\text{CH}_3)$), 1.06 (d, 12 H, $^3J_{\text{HH}} = 6.7$ Hz, $^1\text{Pr}(\text{CH}_3)$). $^{13}\text{C}\{^1\text{H}\}$ NMR (100 MHz, CD₂Cl₂, 25 °C) δ : 147.2 (C₁), 146.2 (d, $^2J_{\text{CP}} = 12$ Hz, C₃), 138.2 (d, $^3J_{\text{CP}} = 6$ Hz, C₂), 133.2 (d, $^3J_{\text{CP}} = 8$ Hz, CH_c), 131.1 (CH_d), 130.4 (CH_b), 129.0 (d, $^1J_{\text{CP}} = 82$ Hz, C₄), 124.8 (CH_a), 119.7 (q, $^1J_{\text{CF}} = 323$ Hz, CF₃), 31.7 ($^1\text{Pr}(\text{CH})$), 25.5 ($^1\text{Pr}(\text{CH}_3)$), 23.1 ($^1\text{Pr}(\text{CH}_3)$), 16.2 (d, $^1J_{\text{CP}} = 36$ Hz, PMe₂). $^{31}\text{P}\{^1\text{H}\}$ NMR (160 MHz, CD₂Cl₂, 25 °C) δ : 4.8.

Compound 4

In an NMR tube, a solution of **1** (30 mg, 0.03 mmol) in CD₂Cl₂ (0.5 mL) was treated with tin(II) chloride (6.0 mg, 0.03 mmol). The tube was shaken resulting in the immediate formation of compound **3**, (17 mg, 48%). Anal. calcd for C₃₄H₄₃AuCl₂F₆NO₄PS₂Sn: C, 36.3; H, 3.9; N, 1.2; S, 5.7. Found: C, 36.3; H, 3.9; N, 1.5; S, 5.5. Spectroscopic data for compound **4-THF**: ^1H NMR (400 MHz, THF-*d*₈, 25 °C) δ : 7.58 (td, 1 H,



$^3J_{\text{HH}} = 7.6$ Hz, $^5J_{\text{HP}} = 1.9$ Hz, H_d), 7.42 (t, 2 H, $^3J_{\text{HH}} = 7.6$ Hz, H_b), 7.29 (dd, 2 H, $^3J_{\text{HH}} = 7.6$ Hz, $^4J_{\text{HP}} = 3.4$ Hz, H_c), 7.25 (d, 4 H, $^3J_{\text{HH}} = 7.6$ Hz, H_a), 2.62 (sept, 4 H, $^3J_{\text{HH}} = 6.7$ Hz, $^1\text{Pr}(\text{CH})$), 1.35 (d, 12 H, $^3J_{\text{HH}} = 7.0$ Hz, $^1\text{Pr}(\text{CH}_3)$), 1.27 (d, 6 H, $^2J_{\text{HP}} = 10.4$ Hz, PMe_2), 1.03 (d, 12 H, $^3J_{\text{HH}} = 7.0$ Hz, $^1\text{Pr}(\text{CH}_3)$). $^{13}\text{C}\{^1\text{H}\}$ NMR (100 MHz, THF-*d*₈, 25 °C) δ : 147.1 (C₁), 145.7 (d, $^2J_{\text{CP}} = 11$ Hz, C₃), 139.4 (d, $^3J_{\text{CP}} = 5$ Hz, C₂), 133.7 (d, $^3J_{\text{CP}} = 8$ Hz, CH_c), 130.2 (CH_d), 130.0 (CH_b), 129.3 (d, $^1J_{\text{CP}} = 56$ Hz, C₄), 124.0 (CH_a), 121.0 (q, $^1J_{\text{CF}} = 320$ Hz, CF₃), 31.9 ($^1\text{Pr}(\text{CH})$), 25.6 ($^1\text{Pr}(\text{CH}_3)$), 23.1 ($^1\text{Pr}(\text{CH}_3)$), 17.9 (d, $^1J_{\text{CP}} = 38$ Hz, PMe_2). $^{31}\text{P}\{^1\text{H}\}$ NMR (160 MHz, THF-*d*₈, 25 °C) δ : -3.1.

Compound 6

A THF (5 mL) solution of **5** (150 mg, 0.22 mmol) was added under argon atmosphere over a solution of :GeCl₂-dioxane (50 mg, 0.22 mmol) in THF (5 mL), then stirred for 30 minutes at room temperature. The solvent was then removed under vacuum to give compound **6** as a fine white powder (161 mg, 88%). Crystals suitable for X-ray studies were grown by slow diffusion of pentane into a dichloromethane solution of **6**. Anal. calcd for C₃₂H₄₃AuCl₃GeP: C, 46.1; H, 5.2. Found: C, 45.8; H, 5.5. ^1H NMR (400 MHz, CD₂Cl₂, 25 °C) δ : 7.58 (td, 1 H, $^3J_{\text{HH}} = 7.6$ Hz, $^5J_{\text{HP}} = 1.6$ Hz, H_d), 7.47 (t, 2 H, $^3J_{\text{HH}} = 7.6$ Hz, H_b), 7.38 (d, 4 H, $^3J_{\text{HH}} = 7.6$ Hz, H_a), 7.24 (dd, 2 H, $^3J_{\text{HH}} = 7.6$ Hz, $^4J_{\text{HP}} = 3.5$ Hz, H_c), 2.48 (sept, 4 H, $^3J_{\text{HH}} = 6.8$ Hz, $^1\text{Pr}(\text{CH})$), 1.36 (d, 12 H, $^3J_{\text{HH}} = 6.8$ Hz, $^1\text{Pr}(\text{CH}_3)$), 1.33 (d, 6 H, $^2J_{\text{HP}} = 10$ Hz, PMe_2), 1.05 (d, 12 H, $^3J_{\text{HH}} = 6.8$ Hz, $^1\text{Pr}(\text{CH}_3)$). $^{13}\text{C}\{^1\text{H}\}$ NMR (100 MHz, CD₂Cl₂, 25 °C) δ : 146.9 (C₁), 146.4 (d, $^2J_{\text{CP}} = 11$ Hz, C₃), 138.1 (d, $^3J_{\text{CP}} = 6$ Hz, C₂), 133.1 (d, $^3J_{\text{CP}} = 7$ Hz, CH_c), 130.8 (CH_d), 130.4 (CH_b), 127.5 (d, $^1J_{\text{CP}} = 52$ Hz, C₄), 124.6 (CH_a), 31.7 ($^1\text{Pr}(\text{CH})$), 25.6 ($^1\text{Pr}(\text{CH}_3)$), 23.1 ($^1\text{Pr}(\text{CH}_3)$), 16.5 (d, $^1J_{\text{CP}} = 33$ Hz, PMe_2). $^{31}\text{P}\{^1\text{H}\}$ NMR (160 MHz, CD₂Cl₂, 25 °C) δ : 5.0.

Compound 7

A THF (5 mL) solution of **5** (150 mg, 0.22 mmol) was added under argon atmosphere over a solution of tin(II) chloride (41 mg, 0.22 mmol) in THF (5 mL), then stirred for 30 minutes at room temperature. The solvent was then removed under vacuum to give compound **7** as a fine white powder (172 mg, 89%). Anal. calcd for C₃₂H₄₃AuCl₃PSn: C, 43.6; H, 4.9. Found: C, 43.5; H, 5.1. ^1H NMR (400 MHz, CD₂Cl₂, 25 °C) δ : 7.56 (td, 1 H, $^3J_{\text{HH}} = 7.6$ Hz, $^5J_{\text{HP}} = 1.8$ Hz, H_d), 7.47 (t, 2 H, $^3J_{\text{HH}} = 7.6$ Hz, H_b), 7.33 (d, 4 H, $^3J_{\text{HH}} = 7.6$ Hz, H_a), 7.24 (dd, 2 H, $^3J_{\text{HH}} = 7.6$ Hz, $^4J_{\text{HP}} = 3.5$ Hz, H_c), 2.52 (sept, 4 H, $^3J_{\text{HH}} = 6.8$ Hz, $^1\text{Pr}(\text{CH})$), 1.35 (d, 12 H, $^3J_{\text{HH}} = 6.8$ Hz, $^1\text{Pr}(\text{CH}_3)$), 1.33 (d, 6 H, $^2J_{\text{HP}} = 10$ Hz, PMe_2), 1.05 (d, 12 H, $^3J_{\text{HH}} = 6.8$ Hz, $^1\text{Pr}(\text{CH}_3)$). $^{13}\text{C}\{^1\text{H}\}$ NMR (100 MHz, CD₂Cl₂, 25 °C) δ : 147.0 (C₁), 146.0 (d, $^2J_{\text{CP}} = 11$ Hz, C₃), 138.7 (d, $^3J_{\text{CP}} = 4$ Hz, C₂), 133.2 (d, $^3J_{\text{CP}} = 7$ Hz, CH_c), 130.5 (CH_d), 130.0 (CH_b), 124.2 (CH_a), 31.7 ($^1\text{Pr}(\text{CH})$), 25.6 ($^1\text{Pr}(\text{CH}_3)$), 23.1 ($^1\text{Pr}(\text{CH}_3)$), 17.4 (d, $^1J_{\text{CP}} = 38$ Hz, PMe_2). The quaternary carbon C₄ could not be located neither in the $^{13}\text{C}\{^1\text{H}\}$ NMR spectrum or by two-dimensional ^1H - ^{13}C correlations. $^{31}\text{P}\{^1\text{H}\}$ NMR (160 MHz, CD₂Cl₂, 25 °C) δ : -2.2.

Compound 8

In an NMR tube, a solution of **5** (30 mg, 0.04 mmol) in C₆D₆ (0.5 mL) was treated with tin(II) bis(trimethylsilyl)amide (19 mg, 0.04 mmol). The tube was shaken resulting in the formation of compound **8** after 5 minutes. The compound could be isolated as a white powder after removing the solvent under reduced pressure (22 mg, 48%).

^1H NMR (400 MHz, C₆D₆, 25 °C) δ : 7.45 (t, 2 H, $^3J_{\text{HH}} = 7.6$ Hz, H_b), 7.24 (d, 4 H, $^3J_{\text{HH}} = 7.6$ Hz, H_a), 7.15 (dd, 2 H, $^3J_{\text{HH}} = 7.6$ Hz, $^4J_{\text{HP}} = 3.5$ Hz, H_c), 6.98 (td, 1 H, $^3J_{\text{HH}} = 7.6$ Hz, $^5J_{\text{HP}} = 1.8$ Hz, H_d), 2.52 (sept, 4 H, $^3J_{\text{HH}} = 6.8$ Hz, $^1\text{Pr}(\text{CH})$), 1.30 (d, 12 H, $^3J_{\text{HH}} = 6.8$ Hz, $^1\text{Pr}(\text{CH}_3)$), 1.10 (d, 6 H, $^2J_{\text{HP}} = 10$ Hz, PMe_2), 0.90 (d, 12 H, $^3J_{\text{HH}} = 6.8$ Hz, $^1\text{Pr}(\text{CH}_3)$), 0.47 (s, $^2J_{\text{HSi}} = 15.3$ Hz, $^4J_{\text{HSn}} = 6.5$ Hz, SiMe₃). $^{13}\text{C}\{^1\text{H}\}$ NMR (100 MHz, C₆D₆, 25 °C) δ : 146.9 (C₁), 146.3 (C₃), 137.8 (d, $^3J_{\text{CP}} = 6$ Hz, C₂), 132.6 (d, $^3J_{\text{CP}} = 7$ Hz, CH_c), 130.7 (CH_d), 129.6 (CH_b), 124.3 (CH_a), 123.2 (d, $^1J_{\text{CP}} = 60$ Hz, C₄), 31.6 ($^1\text{Pr}(\text{CH})$), 25.6 ($^1\text{Pr}(\text{CH}_3)$), 23.2 ($^1\text{Pr}(\text{CH}_3)$), 17.1 (d, $^1J_{\text{CP}} = 30$ Hz, PMe_2), 7.27 ($^1J_{\text{CSi}} = 55$ Hz, $^3J_{\text{CSn}} = 16$ Hz, SiMe₃). $^{31}\text{P}\{^1\text{H}\}$ NMR (160 MHz, C₆D₆, 25 °C) δ : 15.4 ($^2J_{\text{PSn}} = 3201$ Hz).

Compound 9

In an NMR tube, a solution of **1** (30 mg, 0.03 mmol) in C₆D₆ (0.5 mL) was treated with tin(II) bis(trimethylsilyl)amide (14 mg, 0.03 mmol). The tube was shaken resulting in the formation of **9** after 5 minutes. The compound could be isolated as a white powder after removing the solvent under reduced pressure (20 mg, 48%).

^1H NMR (400 MHz, C₆D₆, 25 °C) δ : 7.26 (m, 3 H, H_d, H_b), 7.14 (d, 4 H, $^3J_{\text{HH}} = 7.6$ Hz, H_a), 6.94 (m, 2 H, H_c), 2.56 (sept, 4 H, $^3J_{\text{HH}} = 6.8$ Hz, $^1\text{Pr}(\text{CH})$), 1.58 (d, 6 H, $^2J_{\text{HP}} = 10$ Hz, PMe_2), 1.28 (d, 12 H, $^3J_{\text{HH}} = 6.8$ Hz, $^1\text{Pr}(\text{CH}_3)$), 0.89 (d, 12 H, $^3J_{\text{HH}} = 6.8$ Hz, $^1\text{Pr}(\text{CH}_3)$), 0.47 (s, SiMe₃). $^{13}\text{C}\{^1\text{H}\}$ NMR (100 MHz, C₆D₆, 25 °C) δ : 146.6 (C₁), 145.9 (d, $^2J_{\text{CP}} = 10$ Hz, C₃), 138.3 (d, $^3J_{\text{CP}} = 5$ Hz, C₂), 132.9 (d, $^3J_{\text{CP}} = 7$ Hz, CH_c), 130.0 (CH_d), 129.6 (CH_b), 124.3 (CH_a), 120.0 (q, $^1J_{\text{CF}_3} = 322$ Hz, CF₃), 31.6 ($^1\text{Pr}(\text{CH})$), 25.6 ($^1\text{Pr}(\text{CH}_3)$), 23.2 ($^1\text{Pr}(\text{CH}_3)$), 16.6 (d, $^1J_{\text{CP}} = 33$ Hz, PMe_2), 6.7 ($^1J_{\text{CSi}} = 55$ Hz, $^3J_{\text{CSn}} = 16$ Hz, SiMe₃). $^{31}\text{P}\{^1\text{H}\}$ NMR (160 MHz, C₆D₆, 25 °C) δ : 13.8.

Compound 10

A CH₂Cl₂ (3 mL) solution of **2** (90 mg, 0.15 mmol) was added under argon atmosphere over tin(II) chloride (56 mg, 0.30 mmol) and the resulting red solution was stirred for 5 minutes at room temperature. Compound **10** could be crystallized by slow diffusion of hexane at -30 °C (26 mg, 11%).

^1H NMR (400 MHz, CD₂Cl₂, 25 °C) δ : 6.15 (d, 1 H, $^1J_{\text{HP}} = 452$ Hz, H-P(C(CH₃)₃)), 1.69 (d, 27 H, $^3J_{\text{HP}} = 15.0$ Hz, H-P(C(CH₃)₃)), 1.55 (d, 54 H, $^3J_{\text{HP}} = 13.0$ Hz, Pt-P(C(CH₃)₃)). $^{13}\text{C}\{^1\text{H}\}$ NMR (100 MHz, CD₂Cl₂, 25 °C) δ : 40.5 (vt, $^1J_{\text{CP}} = 7$ Hz, Pt-P(C(CH₃)₃)), 38.0 (d, $^1J_{\text{CP}} = 28$ Hz, H-P(C(CH₃)₃)), 33.6 (Pt-P(C(CH₃)₃)), 30.6 (H-P(C(CH₃)₃)). $^{31}\text{P}\{^1\text{H}\}$ NMR (160 MHz, CD₂Cl₂, 25 °C) δ : 128.3 ($^2J_{\text{PSn}} = 110$ Hz, $^1J_{\text{PPt}} = 4874$ Hz, Pt-P(C(CH₃)₃)), 51.9 (H-P(Bu)₃). UV-vis (CH₂Cl₂) λ_{max} (ϵ [cm⁻¹ M⁻¹]): 572 nm (102).



Compound 13

A solid mixture of compounds **1** (100 mg, 0.106 mmol), **2** (64 mg, 0.106 mmol) and :GeCl₂-dioxane (25 mg, 0.106 mmol) was placed in a Schlenk flask inside a dry box, dissolved in CH₂Cl₂ (5 mL) and stirred at room temperature for 15 minutes. Addition of pentane (10 mL) caused precipitation of **13** as an orange solid that was washed with pentane (150 mg, 92%). This compound can be recrystallized by slow diffusion of pentane into a toluene solution (2 : 1 by vol.) at -20 °C. Anal. calcd for C₅₈H₉₇AuF₆NO₄P₃PtS₂: C, 45.4; H, 6.4; N, 0.9; S, 4.2. Found: C, 45.8; H, 6.2; N, 0.8; S, 4.0. ¹H NMR (400 MHz, CD₂Cl₂, 25 °C) δ: 7.52 (td, 1 H, ³J_{HH} = 7.6 Hz, ⁵J_{HP} = 2.0 Hz, H_d), 7.42 (t, 2 H, ³J_{HH} = 7.6 Hz, H_b), 7.26 (d, 4 H, ³J_{HH} = 7.6 Hz, H_a), 7.14 (dd, 2 H, ³J_{HH} = 7.6 Hz, ⁴J_{HP} = 3.6 Hz, H_c), 2.56 (sept, 4 H, ³J_{HH} = 6.5 Hz, ¹Pr(CH)), 1.50 (vt, 54 H, ³J_{HP} = 6.4 Hz, ^tBu), 1.30 (d, 12 H, ³J_{HH} = 6.7 Hz, ¹Pr(CH₃)), 1.19 (d, 6 H, ²J_{HP} = 10 Hz, PMe₂), 1.00 (d, 12 H, ³J_{HH} = 6.7 Hz, ¹Pr(CH₃)). ¹³C{¹H} NMR (100 MHz, CD₂Cl₂, 25 °C) δ: 146.8 (C₁), 144.4 (d, ²J_{CP} = 10 Hz, C₃), 139.2 (d, ⁵J_{CP} = 3 Hz, C₂), 134.8 (d, ³J_{CP} = 9 Hz, CH_c), 130.0 (CH_b), 129.2 (CH_d), 127.4 (d, ¹J_{CP} = 41 Hz, C₄), 124.1 (CH_a), 120.5 (q, ¹J_{CF} = 323 Hz, CF₃), 39.5 (vt, ¹J_{CP} = 8 Hz, ²J_{CPt} = 20 Hz, Pt-P(C(CH₃)₃), 33.8 (Pt-P(C(CH₃)₃), 31.5 (¹Pr(CH)), 25.9 (¹Pr(CH₃), 23.8 (¹Pr(CH₃), 19.7 (d, ¹J_{CP} = 35 Hz, PMe₂). ³¹P{¹H} NMR (160 MHz, CD₂Cl₂, 25 °C) δ: 94.5 (d, ³J_{PP} = 2, ¹J_{Ppt} = 3159 Hz), -34.2 (t, ³J_{PP} = 2, ²J_{Ppt} = 1984 Hz).

Compound 14

A dichloromethane (5 mL) solution of compound **1** (50 mg, 0.05 mmol) was treated with P^tBu₃ (10.7 mg, 0.05 mmol) under argon atmosphere. The solution was stirred at -80 °C for 5 min and the temperature was slowly raised to 25 °C. Compound **14** was precipitated by the addition of pentane as a white solid that was further washed with the same solvent (49 mg, 86%). ¹H NMR (400 MHz, CD₂Cl₂, 25 °C) δ: 7.60 (td, 1 H, ³J_{HH} = 7.6 Hz, ⁵J_{HP} = 1.7 Hz, H_d), 7.44 (t, 2 H, ³J_{HH} = 7.6 Hz, H_b), 7.31 (d, 4 H, ³J_{HH} = 7.6 Hz, H_a), 7.23 (dd, 2 H, ³J_{HH} = 7.6 Hz, ⁴J_{HP} = 3.4 Hz, H_c), 2.53 (sept, 4 H, ³J_{HH} = 6.8 Hz, ¹Pr(CH)), 1.57 (d, 6 H, ²J_{HP} = 10.4 Hz, PMe₂), 1.35 (d, 27 H, ³J_{HP} = 15 Hz, ^tBu), 1.23 (d, 12 H, ³J_{HH} = 7.0 Hz, ¹Pr(CH₃)), 1.06 (d, 12 H, ³J_{HH} = 7.0 Hz, ¹Pr(CH₃)). ¹³C{¹H} NMR (100 MHz, CD₂Cl₂, 25 °C) δ: 146.6 (C₁), 146.1 (d, ²J_{CP} = 10 Hz, C₃), 137.7 (d, ³J_{CP} = 3 Hz, C₂), 132.9 (d, ⁵J_{CP} = 7 Hz, CH_c), 129.9 (CH_d), 125.2 (CH_b), 123.8 (CH_a), 119.7 (q, ¹J_{CF} = 323 Hz, CF₃), 39.9 (d, ¹J_{CP} = 16 Hz, P(C(CH₃)₃), 32.3 (P(C(CH₃)₃), 31.3 (¹Pr(CH)), 25.0 (¹Pr(CH₃)), 22.9 (¹Pr(CH₃)), 16.0 (d, ¹J_{CP} = 34 Hz, PMe₂). ³¹P{¹H} NMR (160 MHz, CD₂Cl₂, 25 °C) δ: 100.6 (²J_{PP} = 312 Hz), 14.6 (²J_{PP} = 312 Hz).

Compound 15

An NMR tube was charged with PMeXyl₂ (18 mg, 0.075 mmol), Pt(P^tBu₃)₂ (30 mg, 0.05 mmol), tin(II) dichloride (14.4 mg, 0.075 mmol) and deuterated benzene or toluene (0.5 mL). The initial white suspension became a red solution after several hours and was stirred for an overall period of 8 hours (85% NMR yield). HRMS (electrospray, *m/z*): calcd for C₂₉H₄₉P₂Pt:

[M - SnCl₂ + H]⁺ 654.7249, found 654.2952. ¹H NMR (400 MHz, tol-*d*₈, 25 °C) δ: 6.90 (t, 2 H, ³J_{HH} = 7.4 Hz, *p*-C₆H₃), 6.76 (dd, 4 H, ³J_{HH} = 7.4 Hz, ⁴J_{HP} = 3.6 Hz, *m*-C₆H₃), 2.93 (dd, 3 H, ³J_{HPt} = 50.7 Hz, ²J_{HP} = 9.0 Hz, ⁴J_{HP} = 2.5 Hz, PMe), 2.51 (s, 12 H, Me_{Xyl}), 1.15 (d, 27 H, ³J_{HP} = 12.6 Hz, ^tBu). ¹³C{¹H} NMR (100.6 MHz, C₆D₆, 25 °C) δ: 141.6 (d, ²J_{CP} = 9 Hz, *o*-C₆H₃), 134.0 (d, ¹J_{CP} = 48 Hz, *ipso*-C₆H₃), 130.0 (d, ³J_{CP} = 8 Hz, *meta*-C₆H₃), 129.1 (d, ⁴J_{CP} = 2 Hz, *para*-C₆H₃), 39.2 (d, ¹J_{CP} = 13, ²J_{CPt} = 55 Hz, Pt-P(C(CH₃)₃), 32.2 (Pt-P(C(CH₃)₃), 25.1 (d, ³J_{CP} = 7 Hz, Me_{Xyl}), 21.0 (d, ¹J_{CP} = 37 Hz, PMe). ³¹P{¹H} NMR (161.98 MHz, tol-*d*₈, 25 °C) δ: 94.6 (d, ¹J_{Ppt} = 3776 Hz, ²J_{PP} = 299 Hz, ²J_{PSn} = 250 Hz, P^tBu₃), 6.3 (d, ¹J_{Ppt} = 3244 Hz, ²J_{PP} = 299 Hz, PMeXyl). ¹⁹⁵Pt{¹H} NMR (86.16 MHz, tol-*d*₈, 25 °C) δ: -4947 (dd, ¹J_{Ppt} = 3776 Hz, ¹J_{PtP} = 3244 Hz, ¹J_{PtSn} = 3210 Hz).

Compound 16

An NMR tube was charged with PMe₂Ar^{Dtbp}₂ (38.7 mg, 0.075 mmol), compound **2** (30 mg, 0.05 mmol), tin(II) dichloride (14.4 mg, 0.075 mmol) and deuterated benzene or toluene (0.5 mL). The initial white suspension became a red solution after several hours and was stirred for an overall period of one day after which we determined a spectroscopic yield of ca. 50%. HRMS (electrospray, *m/z*): calcd for C₄₈H₇₈P₂Pt: [M - SnCl₂] 912.1584, found 912.5291.

¹H NMR (400 MHz, C₆D₆, 25 °C) δ: 7.27–7.23 (m, 8H, Ar), 7.07 (td, 1H, ³J_{HH} = 7.5 Hz, ⁵J_{HP} = 1.5 Hz, *p*-C₆H₃), 1.98 (dd, 6 H, ²J_{HP} = 10.0 Hz, ⁴J_{HP} = 1.9 Hz, PMe₂), 1.49 (br, 36 H, ^tBu (PMe₂Ar^{Dtbp}₂)), 1.34 (d, 27 H, ³J_{HP} = 12.6 Hz, ^tBu (P^tBu₃)). ¹³C{¹H} NMR (100.6 MHz, C₆D₆, 25 °C) δ: 151.7 (s, *m*-Dtbp), 149.9 (d, ²J_{CP} = 10 Hz, *o*-C₆H₃), 141.7 (d, ³J_{CP} = 4 Hz, *ipso*-Dtbp), 131.7 (d, ¹J_{CP} = 8 Hz, *ipso*-C₆H₃), 130.7 (d, ⁴J_{CP} = 7 Hz, *m*-C₆H₃), 127.8 (*p*-C₆H₃), 124.6 (s, *o*-Dtbp), 121.6 (s, *p*-Dtbp), 39.6 (d, ¹J_{CP} = 12, ²J_{CPt} = 42 Hz, Pt-P(C(CH₃)₃), 34.8 (s, C(CH₃)), 32.4 (Pt-P(C(CH₃)₃), 31.9 (s, C(CH₃)), 19.5 (d, ¹J_{CP} = 36 Hz, PMe₂). ³¹P{¹H} NMR (161.98 MHz, C₆D₆, 25 °C) δ: 97.3 (d, ¹J_{Ppt} = 3788 Hz, ²J_{PP} = 307 Hz, ²J_{PSn} = 255 Hz, P^tBu₃), 12.6 (d, ¹J_{Ppt} = 3504 Hz, ²J_{PP} = 307 Hz, PAR^{tBu}). ¹⁹⁵Pt{¹H} NMR (86.16 MHz, C₆D₆, 25 °C) δ: -5067 (dd, ¹J_{Ppt} = 3788 Hz, ¹J_{PtP} = 3504 Hz).

Conclusion

In summary, we have analyzed the reactivity of tin and germanium dihalides with a transition metal-only frustrated Lewis pair based on Pt(0) and Au(I) fragments. Our results reveal a dissimilar reactivity of the tetrylenes in the presence of the two metals compared to the reactions displayed with the individual Au(I) and Pt(0) monometallic species. While the insertion chemistry of :GeCl₂ and :SnCl₂ into Au-X bonds is analogous to prior studies, their reactivity with [Pt(P^tBu₃)₂] (**2**) contrasts with previous work based on less hindered phosphines. As such, we have demonstrated that :SnCl₂ promotes phosphine exchange reactions at Pt(0) centres to access uncommon heteroleptic diphosphine platinum(0) compounds. In addition, an unusual highly-reduced heteropolymetallic aggregate containing a Pt₂Sn₃ core has been isolated and characterized by



X-ray diffraction techniques, while its bonding scheme has been analyzed by computational methods. The different reactivity exhibited by :GeCl₂ compared to :SnCl₂ is also apparent by their addition to the Au(I)/Pt(0) pair. In the former case a metal-only Pt → Au Lewis adduct is readily produced, while in the latter experiment a cationic heteroleptic diphosphine gold compound is the major species.

Conflicts of interest

There are no conflicts to declare.

Acknowledgements

This work has been supported by the European Research Council (ERC Starting Grant, CoopCat, Project 756575). J. J. M. thanks the Universidad de Sevilla for a research grant. The use of computational facilities at the Supercomputing Centre of Galicia (CESGA) is acknowledged. We are grateful to J. López-Serrano, M. Roselló, F. Molina, Francisco F. de Córdoba and Eleuterio Alvarez for valuable discussions.

References

- 1 E. Rivard, *Dalton Trans.*, 2014, **43**, 8577.
- 2 (a) T. J. Marks, *J. Am. Chem. Soc.*, 1971, **93**, 7090; (b) T. J. Marks and A. R. Newman, *J. Am. Chem. Soc.*, 1973, **95**, 769; (c) C. Eisenhut, T. Szilvasi, G. Dübek, N. C. Breit and S. Inoue, *Inorg. Chem.*, 2017, **56**, 10061; (d) S. K. Grumbine, D. A. Straus, T. D. Tilley and A. L. Rheingold, *Polyhedron*, 1995, **14**, 127.
- 3 (a) M. Y. Abraham, Y. Wang, Y. Xie, P. Wei, H. F. Schaefer, P. v. R. Schleyer and G. H. Robinson, *J. Am. Chem. Soc.*, 2011, **133**, 8874; (b) K. C. Thimer, S. M. I. Al-Rafia, M. J. Ferguson, R. McDonald and E. Rivard, *Chem. Commun.*, 2009, 7119; (c) A. K. Swarnakar, S. M. McDonald, K. C. Deutsch, P. Choi, M. J. Ferguson, R. McDonald and E. Rivard, *Inorg. Chem.*, 2014, **53**, 8662; (d) S. M. I. Al-Rafia, A. C. Malcolm, S. K. Liew, M. J. Ferguson and E. Rivard, *J. Am. Chem. Soc.*, 2011, **133**, 777; (e) S. M. I. Al-Rafia, O. Shynkaruk, S. M. McDonald, S. K. Liew, M. J. Ferguson, R. McDonald, R. H. Herber and E. Rivard, *Inorg. Chem.*, 2013, **52**, 5581.
- 4 (a) R. S. Ghadwal, H. W. Roesky, S. Merkel and D. Stalke, *Chem. – Eur. J.*, 2010, **16**, 85; (b) R. Azhakar, G. Tavcar, H. W. Roesky, J. Hey and D. Stalke, *Eur. J. Inorg. Chem.*, 2011, 475; (c) S. M. I. Al-Rafia, A. C. Malcolm, R. McDonald, M. J. Ferguson and E. Rivard, *Chem. Commun.*, 2012, **48**, 1308; (d) R. S. Ghadwal, R. Azhakar, K. Pröpper, J. J. Holstein, B. Dittrich and H. W. Roesky, *Inorg. Chem.*, 2011, **50**, 8502.
- 5 (a) J. A. Cabeza, P. García-Álvarez and D. Polo, *Eur. J. Inorg. Chem.*, 2016, 10; (b) M. F. Lappert and R. S. Rowe, *Coord. Chem. Rev.*, 1990, **100**, 267; (c) W. Petz, *Chem. Rev.*, 1986, **86**, 1019.
- 6 (a) D. W. Stephan and G. Erker, *Angew. Chem., Int. Ed.*, 2015, **54**, 6400; (b) D. W. Stephan and G. Erker, *Top. Curr. Chem.*, 2013, **334**, 1; (c) D. W. Stephan and G. Erker, *Top. Curr. Chem.*, 2013, **332**, 1; (d) D. W. Stephan and G. Erker, *Angew. Chem., Int. Ed.*, 2010, **49**, 46; (e) D. W. Stephan, *J. Am. Chem. Soc.*, 2015, **137**, 10018; (f) D. W. Stephan, *Science*, 2016, **354**, 1248.
- 7 (a) B. Michelet, C. Bour and V. Gandon, *Chem. – Eur. J.*, 2014, **20**, 14488; (b) J. A. B. Abdalla, I. M. Riddlestone, R. Tirfoin and S. Aldridge, *Angew. Chem., Int. Ed.*, 2015, **54**, 5098; (c) J. Backs, M. Lange, J. Possart, A. Wollschlager, C. Muck-Lichtenfeld and W. Uhl, *Angew. Chem., Int. Ed.*, 2017, **56**, 3094; (d) Y. Yu, J. Li, W. Liu, O. Yeb and H. Zhu, *Dalton Trans.*, 2016, **45**, 6259.
- 8 (a) A. Jana, I. Objartel, H. W. Roesky and D. Stalke, *Inorg. Chem.*, 2009, **48**, 7645; (b) A. Jana, G. Tavčar, H. W. Roesky and C. Schulzke, *Dalton Trans.*, 2010, **39**, 6217.
- 9 J. Campos, *J. Am. Chem. Soc.*, 2017, **139**, 2944.
- 10 A. K. Swarnakar, M. J. Ferguson, R. McDonald and E. Rivard, *Dalton Trans.*, 2016, **45**, 6071.
- 11 (a) H. Yang, J. Zhao, M. Qiu, P. Sun, D. Han, L. Niu and G. Cui, *Biosens. Bioelectron.*, 2019, **124–125**, 191; (b) L. Wang, E. Guan, J. Zhang, J. Yang, Y. Zhu, Y. Han, M. Yang, C. Cen, G. Fu, B. C. Gates and F.-S. Xiao, *Nat. Commun.*, 2018, **9**, 1362.
- 12 (a) A. Aouissi, S. S. Al-Deyab and H. Al-Shahri, *Molecules*, 2010, **15**, 1398; (b) B. Pan and F. P. Gabbaï, *J. Am. Chem. Soc.*, 2014, **136**, 9564.
- 13 M. F. Espada, J. Campos, J. López-Serrano, M. L. Poveda and E. Carmona, *Angew. Chem., Int. Ed.*, 2015, **54**, 15379.
- 14 (a) A. Bauer, A. Schier and H. Schmidbaur, *J. Chem. Soc., Dalton Trans.*, 1995, 2919; (b) A. Bauer and H. Schmidbaur, *J. Am. Chem. Soc.*, 1996, **118**, 2919; (c) J. A. Dilts and M. P. Johnson, *Inorg. Chem.*, 1966, **5**, 2079; (d) D. M. Mingos, H. R. Powell and T. L. Stolberg, *Transition Met. Chem.*, 1992, **17**, 334.
- 15 (a) R. V. Bojan, J. M. López-de-Luzuriaga, M. Monge, M. E. Olmos, R. Echeverría, O. Lehtonen and D. Sundholm, *ChemPlusChem*, 2016, **81**, 176; (b) R. V. Bojan, J. M. López-de-Luzuriaga, M. Monge, M. E. Olmos, R. Echeverría, O. Lehtonen and D. Sundholm, *ChemPlusChem*, 2014, **79**, 67.
- 16 P. Pérez-Galán, N. Delpont, E. Herrero-Gómez, F. Maseras and A. M. Echavarren, *Chem. – Eur. J.*, 2010, **16**, 5324.
- 17 (a) U. Anandhi and P. R. Sharp, *Inorg. Chim. Acta*, 2006, **359**, 3521; (b) J. A. Cabeza, J. M. Fernández-Colinas, P. García-Álvarez and D. Polo, *Inorg. Chem.*, 2012, **51**, 3896; (c) M. Walewska, J. Hlina, W. Gaderbauer, H. Wagner, J. Baumgartner and C. Marschner, *Z. Anorg. Allg. Chem.*, 2016, **642**, 1304.
- 18 (a) J. Hlina, H. Arp, M. Walewska, U. Florke, K. Zangger, C. Marschner and J. Baumgartner, *Organometallics*, 2014, **33**, 7069; (b) B. Findeis, M. Contel, L. H. Gade, M. Laguna, M. C. Gimeno, I. J. Scowen and M. McPartlin, *Inorg. Chem.*,



- 1997, **36**, 2386; (c) C. Marschner, J. Baumgartner, H. Arp, K. Rasmussen, N. Siraj, P. Zark and T. Muller, *J. Am. Chem. Soc.*, 2013, **135**, 7949.
- 19 (a) S. D. Bunge, O. Just and W. S. Rees Jr., *Angew. Chem., Int. Ed.*, 2000, **39**, 3082; (b) K. Angermaier and H. Schmidbauer, *Chem. Ber.*, 1995, **128**, 817; (c) A. Shiotani and H. Schmidbauer, *J. Am. Chem. Soc.*, 1970, **92**, 7003; (d) S. D. Bunge and J. L. Steele, *Inorg. Chem.*, 2009, **48**, 2701.
- 20 (a) F. Hupp, M. Ma, F. Kroll, J. O. C. Jimenez-Halla, R. D. Dewhurst, K. Radacki, A. Stasch, C. Jones and H. Braunschweig, *Chem. – Eur. J.*, 2014, **20**, 16888; (b) H. Braunschweig, M. A. Celik, R. D. Dewhurst, M. Heid, F. Huppa and S. S. Sen, *Chem. Sci.*, 2015, **6**, 425.
- 21 (a) H. Braunschweig, K. Gruss and K. Radacki, *Angew. Chem., Int. Ed.*, 2007, **46**, 7782; (b) J. Bauer, H. Braunschweig, P. Brenner, K. Kraft, K. Radacki and K. Schwab, *Chem. – Eur. J.*, 2010, **16**, 11985.
- 22 T. Yoshida and S. Otsuka, *J. Am. Chem. Soc.*, 1977, **99**, 2134.
- 23 G. W. Bushnell, D. T. Eadie, A. Pidcock, A. R. Sam, R. D. Holmes-Smith and S. R. Stobart, *J. Am. Chem. Soc.*, 1982, **104**, 5837.
- 24 Z. Béni, R. Scopelliti and R. Roulet, *Inorg. Chem. Commun.*, 2005, **8**, 99.
- 25 J. Pipek and P. G. Mezey, *J. Chem. Phys.*, 1989, **90**, 4916.
- 26 J. Bauer, H. Braunschweig and R. D. Dewhurst, *Chem. Rev.*, 2012, **112**, 4329.
- 27 See for example: (a) Y. Liu, F. Song and S. Guo, *J. Am. Chem. Soc.*, 2006, **128**, 11332; (b) F. Inagaki, C. Matsumoto, Y. Okada, N. Maruyama and C. Mukai, *Angew. Chem., Int. Ed.*, 2015, **54**, 818; (c) K. J. Kilpin, W. Henderson and B. K. Nicholson, *Dalton Trans.*, 2008, 3899; (d) J. Zhang, C.-G. Yang and C. He, *J. Am. Chem. Soc.*, 2006, **128**, 1798.
- 28 J. Bauer, H. Braunschweig, A. Damme and K. Radacki, *Angew. Chem., Int. Ed.*, 2012, **51**, 10030.
- 29 (a) S. Arndt, M. M. Hansmann, P. Motloch, M. Rudolph, F. Rominger and A. S. K. Hashmi, *Chem. – Eur. J.*, 2017, **23**, 2542; (b) R. Uson, J. Gimeno, J. Fornies, F. Martinez and C. Fernandez, *Inorg. Chim. Acta*, 1982, **63**, 91; (c) H. El-Amouri, A. A. Bahsoun, J. Fischer, J. A. Osborn and M.-T. Youinou, *Organometallics*, 1991, **10**, 3582.
- 30 (a) M. Devillard, R. Declercq, E. Nicolas, A. W. Ehlers, J. Backs, N. Saffon-Merceron, G. Bouhadir, J. C. Slootweg, W. Uhl and D. Bourissou, *J. Am. Chem. Soc.*, 2016, **138**, 4917; (b) B. E. Cowie, F. A. Tsao and D. J. H. Emslie, *Angew. Chem., Int. Ed.*, 2015, **54**, 2165.
- 31 J. Bauer, H. Braunschweig, P. Brenner, K. Kraft, K. Radacki and K. Schwab, *Chem. – Eur. J.*, 2010, **16**, 11985.
- 32 (a) J. Campos, R. Peloso and E. Carmona, *Angew. Chem., Int. Ed.*, 2012, **51**, 8255; (b) J. Campos, L. Ortega-Moreno, S. Conejero, R. Peloso, J. López-Serrano, C. Maya and E. Carmona, *Chem. – Eur. J.*, 2015, **21**, 8883; (c) M. Marín, J. J. Moreno, C. Navarro-Gilabert, E. Álvarez, C. Maya, R. Peloso, M. C. Nicasio and E. Carmona, *Chem. – Eur. J.*, 2019, **25**, 260.
- 33 (a) R. R. Sharp and J. W. Tolan, *J. Chem. Phys.*, 1976, **65**, 522; (b) R. R. Sharp, *J. Chem. Phys.*, 1972, **57**, 5321.
- 34 J. Campos, M. F. Espada, J. López-Serrano and E. Carmona, *Inorg. Chem.*, 2013, **52**, 6694.
- 35 (a) K. Wolinski, J. F. Hinton and P. Pulay, *J. Am. Chem. Soc.*, 1990, **112**, 8251; (b) M. Häser, R. Ahlrichs, H. P. Baron, P. Weiss and H. Horn, *Theor. Chim. Acta*, 1992, **83**, 455.
- 36 A. Uson, M. Laguna, D. A. Briggs, H. H. Murray and J. P. Fackler, *Inorg. Synth.*, 2007, **26**, 85.
- 37 H.-R. C. Jaw and W. R. Mason, *Inorg. Chem.*, 1989, **28**, 4310.

